# Transport of Particles and Impurities in DIII–D Discharges with Internal Regions of Enhanced Confinement

D.R. Baker,[1] M.R. Wade,[2] L.R. Baylor[2], J.C. DeBoo,[1] C.M. Greenfield,[1] W.A. Houlberg,[2] and B.W. Stallard[3]

[1]General Atomics, P.O. Box 85608, San Diego, California 92186-5608, USA
email: baker@fusion.gat.com
[2]Oak Ridge National Laboratory, Oak Ridge, Tennessee 37381, USA
[3]Lawrence Livermore National Laboratory, Livermore, California 94550, USA

**Abstract**. In DIII–D discharges with centrally enhanced confinement and peaked density profiles there is an accumulation and peaking of impurities in the core, as is predicted by neoclassical theory. In VH–mode discharges with an outer region of enhanced confinement and a broad density profile, the neoclassical thermal screening effect causes the impurities to accumulate near the edge. In discharges with anomalously high transport, the measured particle diffusivities are close to the measured thermal diffusivities and the density profiles are proportional to a fractional power of 1/q. When the plasma has regions of enhanced confinement, where the ion thermal transport is near neoclassical, then the particle transport also exhibits neoclassical transport behavior such as low diffusivities, neoclassical pinch effects and ion temperature gradient screening. Here we present experimental results of both impurity and electron transport in DIII–D discharges with large internal regions of enhanced confinement and discuss the relevance of these results to future tokamak designs.

## 1. Introduction

DIII–D discharges with internal regions of enhanced energy confinement also have regions of enhanced particle confinement. Enhanced core particle confinement has both deleterious and beneficial effects on the plasma performance, and the understanding and control of the particle transport and density profiles is key to optimizing the performance in steady-state Advanced Tokamak discharges. Discharges with significant reduction in core turbulence, where neoclassical particle transport becomes important, should have density profiles as broad as possible to optimize fusion performance and minimize the accumulation of impurities.

## 2. High Transport Profiles – L–mode and Standard ELMy H–mode

In DIII–D plasmas with anomalously high transport, the electron density profile is approximately proportional to $(q\mathsf{H})^{\xi}$, as shown in Fig. 1. Here q is the usual tokamak safety factor and $\mathsf{H}$ is a geometric term proportional to $dV/d\Phi$, where V is the plasma volume and $\Phi$ is the toroidal magnetic flux. The safety factor is measured by a 36 channel Motional Stark Effect diagnostic which includes a correction for the radial electric field. In standard L–mode $\xi \approx 0.8$ and in standard ELMy H–mode $\xi \approx 0.3$. These profiles result from a balance of an outward diffusion term and an inward anomalous pinch [1]. In these standard type of anomalously transporting plasmas the impurity density profiles are proportional to the electron density profiles [2]. In this paper “standard” refers to discharges without central regions of enhanced confinement and without special treatment of the edge or pumping of the edge for the purpose of modifying the ELMs or enhancing confinement. In standard L–mode, in addition to controlling the density profile by controlling the q profile, the density profiles can be modified somewhat by varying the relative amounts of beam fueling compared to gas puffing. However, independent control of the average density and the profile shape in L–modes is not usually possible using fueling techniques alone. In standard ELMy H–mode the profiles are relatively flat and the average density is determined by a combination of wall recycling, gas puffing and beam fueling.

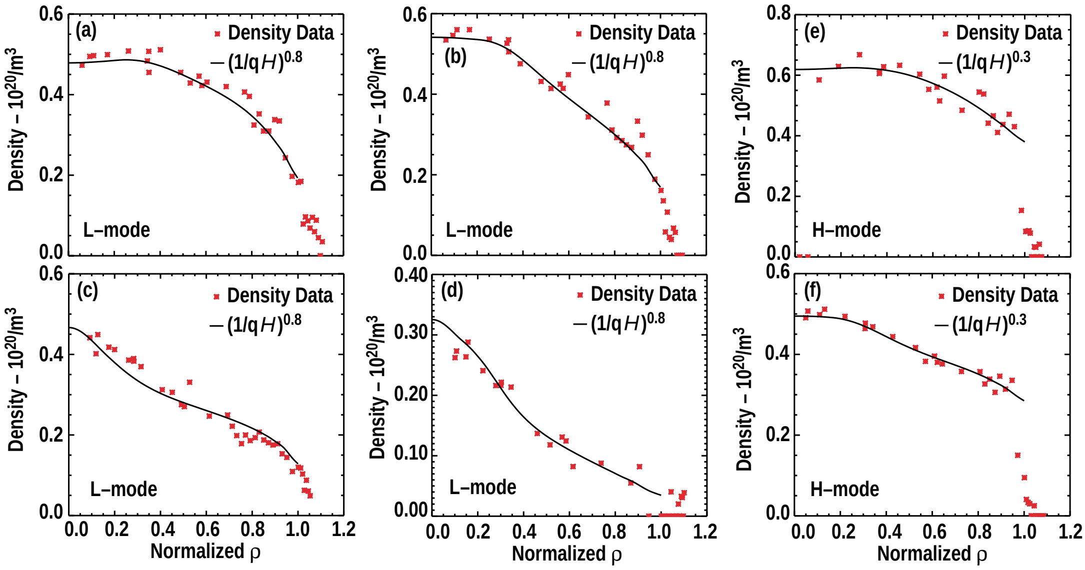


*FIG. 1. Density profiles for different q profiles. The different shapes of the q profile are obtained by ramping the plasma current up and then down. The data points are from Thomson scattering. L–mode (a–d), the line is a plot of (q**H**)$^{-0.8}$ fitted to the density at ρ = 0.6. H–mode (e-f), the line is a plot of (q**H**)$^{-0.3}$ fitted to density of ρ=0.6.*

## 3. Enhanced Confinement Profiles

### 3.1. Internal Transport Barriers

#### 3.1.1. Electrons

Concurrent with an internal transport barrier (ITB) in the ion thermal channel, there is a peaking of the electron density, which is mainly due to the good confinement of the thermalized central beam particle source [3]. As shown in Fig. 2, in the central region, where the ion thermal diffusivities approach neoclassical values, the electron particle diffusivities become small and at the very center they also approach neoclassical values. In the center of these plasmas it is necessary to account for the neoclassical Ware pinch, otherwise the calculated particle diffusion coefficients can be less than the neoclassical coefficients.

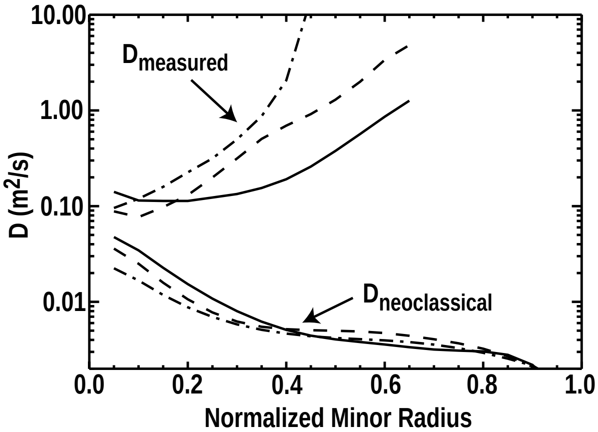


*FIG. 2. Measured electron particle diffusivities for three different discharges with central ITBs compared with the corresponding Chang-Hinton neoclassical values.*

### 3.1.2. Impurities

The peaked electron density profiles in these ITB discharges, show a preferential peaking of medium weight impurities.The neoclassical impurity flux can be expressed by [4–6],

$$\Gamma_z^{neo} = D_{neo}\nabla n_z + n_z D_{neo}\left\{\sum_j g_{j\to z}\frac{\nabla n_j}{n_j} + g_{T_i}\frac{\nabla T_i}{T_i} + g_{T_e}\frac{\nabla T_e}{T_e}\right\} \quad . \tag{1}$$

The parameters $g_{j\to z}$, $g_{Ti}$, $g_{Te}$ depend on the details of momentum transfer between the different particle species and thus depend on local plasma conditions. In the banana regime $g_{e\to z}$ and $g_{Te}$ can be neglected and in steady state, with $\Gamma \to 0$, Eq. (1) reduces to,

$$\frac{n_z(\rho)}{n_z(0)} = \left[\frac{n_D(\rho)}{n_D(0)}\right]^{g_{D\to Z}} \left[\frac{T_i(\rho)}{T_i(0)}\right]^{g_{T_i}} \quad , \tag{2}$$

where ρ is the minor radial coordinate. In many discharges, $g_{D\to Z} >> g_{Ti}$, and then plasmas with peaked main ion density profiles will exhibit an accumulation of impurities in the plasma center, regardless of the ion temperature profiles. This effect has been previously experimentally verified [7]. As shown in Fig. 3(a), this effect has also been seen in DIII–D. Light impurities such as helium have density profiles approximately proportional to the electron density profile, however heavier impurities such as carbon or neon are more peaked as predicted Eq. (2). The data in Fig. 3 is less peaked than predicted by Eq. (2) since the experimental transport is not purely neoclassical.

### 3.2. VH –mode

It can be seen from Eq. (2) that if the deuterium profiles are relatively flat, the shape of the impurity profile can depend on the ion temperature profile. If the impurities and the main ions are in the banana regime then $g_{Ti}$ is usually negative and the impurities are kept to the outer part of the plasma. This is known as temperature screening [4].

The broader density profiles shown in Fig. 3(b) are from DIII–D VH–mode plasmas, which have an extended edge region of enhanced confinement. This region also has near neoclassical levels of transport. In the very outer region of the plasma the ion thermal diffusivities are close to neoclassical levels and the electron particle flux becomes very low. The electron particle diffusivities, although greater than the (very low) neoclassical values, are much lower than the usual anomalous values. The ion particle diffusivities, measured by

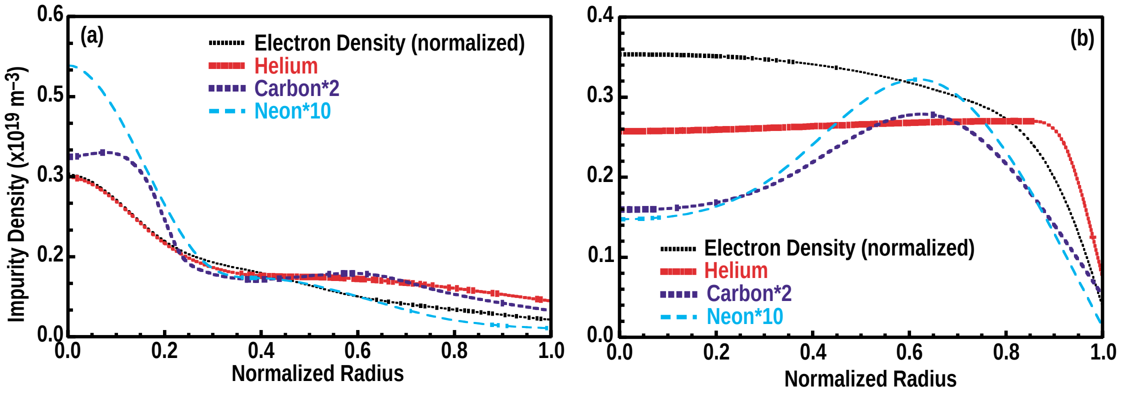


*FIG. 3. (a) Impurities accumulate and peak in the plasma core in discharges with peaked density profiles. (b) Broad density profiles and high ion temperature gradients screen impurities causing them to build up at the edge.*

injecting trace amounts of gases such as helium, neon or nitrogen, are close to, but above, the neoclassical values. These plasmas have steep centrally peaked ion temperature profiles. For these plasmas with broad, flat density profiles and centrally peaked ion temperature profiles, there can be a screening of impurities as indicated by Eq. (2). The impurities then accumulate near the outside of the discharge, Fig. 3(b), where they are more easily removed. In calculating the amount of impurity screening, it is necessary to include the effect of the anomalous pinch and diffusive terms in the evaluation of the total particle flux. The broader density profile is consistent with the stability requirements of broad pressure profile and good alignment of the bootstrap current in Advanced Tokamak plasmas.

## 4. Summary

Although the understanding of particle transport in tokamaks is not complete, the experimental evidence is clear. In DIII–D discharges with anomalously high transport, the measured particle diffusivities are close to the measured thermal diffusivities. The total particle flux, which can be small, consists of anomalously large outward diffusive and inward convection components. Impurities such as helium, carbon, neon or argon show no strong tendency to accumulate in any local region, i.e., $n_Z \propto n_e$. When the plasma has regions of enhanced confinement, where the ion thermal transport becomes close to neoclassical, then the particle transport also shows neoclassical transport behavior such as low diffusivities, and neoclassical pinch terms such as the Ware pinch and central high Z impurity accumulation or thermal screening, depending on the shape of the density profile.

In light of the above particle transport understanding, a reacting tokamak should have a broad density profile, which experimentally has been found to be consistent with a broad current profile and also consistent with good bootstrap alignment. This profile shape will minimize the tendency of impurities to accumulate in the center in both anomalous and neoclassical transport regimes. The enhanced confinement region should not be concentrated in the plasma center or have the form of a narrow barrier, but should be broad and perhaps extend out to the plasma boundary. This is consistent with good overall confinement and global stability requirements.


## Acknowledgment

Work supported by U.S. Department of Energy under Contracts DE-AC03-99ER54463, W-7405-ENG-48, and DE-AC05-96OR22725.


## References


[1] BAKER, D.R., WADE, M.R., PETTY, C.C., *et.al.*, Nucl. Fusion **40** (2000) 1003.
[2] WADE, M.R., *et al.*, Proc. of the 23rd EPS Conference on Controlled Fusion and Plasma Physics, Kiev, 1996 (European Physical Society, 1997) Vol. 1. p. 283.
[3] RICE, B.W., BURRELL, K.H., LAO, L.L., *et al.*, Phys. Plasmas **3** (1996) 1983.
[4] RUTHERFORD, P.H., Phys. Fluids **17** (1974) 1782.
[5] HINTON, F.L. and MOORE, T.B., Nucl. Fusion **14** (1974) 639.
[6] HIRSHMAN, S.P., D.J. Sigmar and J.F. Clarke, Phys Fluids **19** (1976) 656.
[7] MILORA, S.L., *et. al.*, Nucl. Fusion **35** (1995) 657.